DOI: 10.1002/ejic.200900736

Formation of Metastable Na_2CrO_4-Type $LiNiPO_4$ from a Phosphate–Formate Precursor

Violeta Koleva,*[a] Radostina Stoyanova,[a] and Ekaterina Zhecheva[a]

Keywords: Lithium / Nickel / Organic–inorganic hybrid composites / Metastable compounds / X-ray diffraction

High-pressure modification of $LiNiPO_4$ with a Na_2CrO_4-type structure was obtained at ambient pressure and low temperature from a mixed LiNi–phosphate–formate precursor, $LiNiPO_4H_x(HCOO)_x{\cdot}yH_2O$ (where $x \approx 1.2$ and $y \approx 2.5$). The structural and thermal characterization of the precursor and the $LiNiPO_4$ compositions were carried out by powder XRD analysis, IR spectroscopy, and DSC analysis. Thermal treatment of $LiNiPO_4H_x(HCOO)_x{\cdot}yH_2O$ precursors between 450 and 650 °C yields a mixture of the two structural modifications of $LiNiPO_4$: the Na_2CrO_4 type and the olivine type. It was established that the obtained Na_2CrO_4-type $LiNiPO_4$ is a metastable phase, which completely transforms at 700 °C into the olivine-type phase. The enthalpy of the phase transition is $\Delta H = -43.40\ \mathrm{kJ\,mol^{-1}}$. The mechanism of formation of the two forms of $LiNiPO_4$ from the LiNi–phosphate–formate precursor is discussed.

Introduction

Lithium transition-metal orthophosphates with the general formula $LiMPO_4$ (M = Fe, Ni, and Co) exhibit three structural modifications. The stable modification at ambient pressure adopts the olivine-type structure. This structure can be described as hexagonal oxygen close packing, where lithium and transition-metal ions occupy half of the available octahedral sites with C_i and C_s symmetry, respectively. The MO_6 octahedra are ordered in a way to form zigzag chains in the *bc* plane, which are cross-linked by PO_4^{3-} groups. Lithium ions fall in the rows (running along the *a* direction) between the transition metal chains. The lithium arrangement in the olivine structure favors the 1D mobility of the Li^+ ions along the *a* direction.[1] The ability of the olivine structure to intercalate and deintercalate lithium reversibly determines phosphoolivines as potential cathode materials for lithium-ion batteries.[2,3] The best electrochemical performance is achieved with the iron analogues, $LiFePO_4$. The reversible electrochemical intercalation of Li^+ from the olivine structure takes place concomitantly with the oxidation/reduction of M^{2+}/M^{3+} ions. This allows manipulating the potential, where Li intercalation takes place, replacing iron by manganese, cobalt, and nickel.[4–6]

The second structural modification of $LiMPO_4$ possesses a spinel-type structure.[7] While the olivine modification is stable at ambient pressure, the spinel modification is formed under high pressures (above 20 GPa) only.

At an intermediate pressure (between 4 and 20 GPa), a new structural modification of $LiMPO_4$ with a Na_2CrO_4-like structure (denoted also as β′-phase in [8]) has been obtained by Amador et al.[7,8] The Na_2CrO_4-like structure consists of layers with the composition $[(MO_6)(LiO_4)(PO_4)]_\infty$ in the *ac* plane, where every MO_6 octahedron shares two opposite edges with neighboring MO_6 and two apical oxygen atoms with two LiO_4 and two PO_4 tetrahedra. Contrary to the olivine-type structure, Li^+ ions occupy isolated tetrahedral positions, as a result of which the lithium mobility is hindered. This determines the lack of electrochemical activity of the Na_2CrO_4-type structure. On the basis of first-principle calculations at the DFT level, it is calculated that, for the Co analogue, both structural modifications possess close to total energies, with an enthalpy difference of 0.05 eV/f.u.[7] However, to the best of our knowledge, there is no data on the preparation of a Na_2CrO_4-type modification at ambient pressure of Fe, Ni, or Co analogues.

In this paper, the preparation of Na_2CrO_4-type modification of the Ni analogue from the LiMPO4 family at ambient pressure is reported. The method of synthesis is based on the formation of metal–organic precursors, where Li^+ and Ni^{2+} ions are bonded by PO_4^{3-} and $HCOO^-$ anions. Metal–organic precursors are isolated by freeze drying aqueous solutions of Li^+, M^{2+}, PO_4^{3-}, and $HCOO^-$ ions. At ambient pressure the thermal decomposition of metal–organic precursors yields a Na_2CrO_4-type modification of $LiNiPO_4$. This method was recently applied to the preparation of $LiFePO_4$ compositions. A pure olivine modification of $LiFePO_4$ is only obtained at ambient pressure.[9] The structural characterization of the $LiNiPO_4$ samples was carried out by powder X-ray diffraction (XRD) analysis and

---

[a] Institute of General and Inorganic Chemistry,
Bulgarian Academy of Sciences,
Acad. G. Bonchev St, bl. 11, 1113 Sofia, Bulgaria
Fax: +359-2-8705024
E-mail: vkoleva@svr.igic.bas.bg

IR spectroscopy. The thermal stability of the Na_2CrO_4-type modification of $LiNiPO_4$ was determined by differential scanning calorimetry (DSC) analysis.

Results and Discussion

Freeze drying solutions containing $Ni(HCOO)_2{\cdot}2H_2O$ and LiH_2PO_4 yields amorphous, pale-green powders with a $LiNiPO_4H_x(HCOO)_x{\cdot}yH_2O$ composition ($x \approx 1.2$ and $y \approx 2.5$), where the Ni(Li) to HCOO ratio decreases from 1:2 to 1:1. This indicates that about 0.8 mol of formic acid is sublimated during the freeze-drying process. The same process of sublimation of formic acid was observed when iron and manganese phosphate–formate precursors are obtained.[9,10]

To rationalize the coordination of formate and phosphate groups, IR spectroscopy was undertaken (Figure 1). For the sake of comparison, the same figure shows the IR spectra of $Ni(HCOO)_2{\cdot}2H_2O$ and $Ni(H_2PO_4)_2{\cdot}2H_2O$.

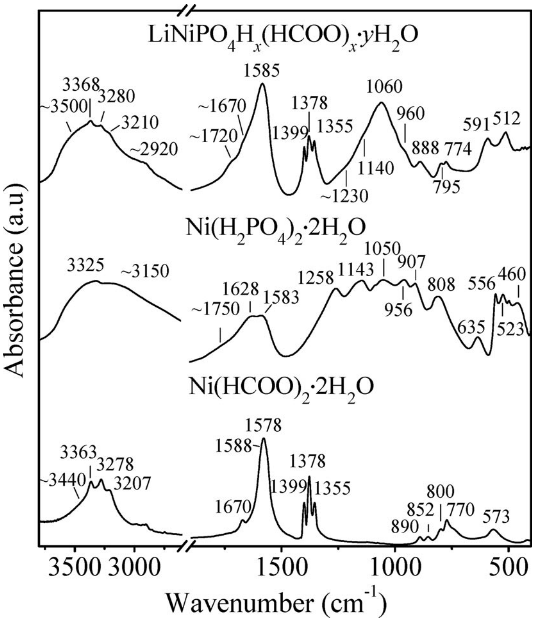

Figure 1. IR spectra of LiNi–phosphate–formate precursor, $Ni(HCOO)_2{\cdot}2H_2O$, and $Ni(H_2PO_4)_2{\cdot}2H_2O$.

In the IR spectra of LiNi–phosphate–formate precursors, the IR modes due to the formate, phosphate, and OH groups are clearly resolved. The characteristic IR bands for the formate ion vibrations are assigned on the basis of IR studies of formate salts.[11–13] These vibrations are: ν_{as}(COO) at 1585 cm^{-1}; δ(CH) at 1399 cm^{-1}; ν_s(COO) at 1378/1355 cm^{-1}, and δ_s(OCO) at 795/774 cm^{-1}. Further on, the δ(CH) and ν_s(COO) vibrations in the Ni precursor are the same as those detected for pure $Ni(HCOO)_2{\cdot}2H_2O$. Therefore, one can suppose that the formate ions are preferentially coordinated around the Ni^{2+} ions in LiNi precursors.

In addition, the low intensity of the IR bands at 960, 1230, and 1720 cm^{-1} cannot be unambiguously attributed. In this region, the characteristic bands for protonated HCOOH groups appear: ν(C=O) at about 1700 cm^{-1}, ν(C–O) at 1260 cm^{-1}, and γ(OH) at 975 cm^{-1}.[15] The protonated phosphate ions such as $H_2PO_4^-$ or HPO_4^{2-} also display bands at 1230–1260 and 800–900 cm^{-1} due to out-of-plane δ(OH) and in-plane γ(OH) bending POH vibrations, respectively.[16,17] Close inspection of the IR spectra of LiNi precursors, $Ni(HCOO)_2{\cdot}2H_2O$, and $Ni(H_2PO_4)_2{\cdot}2H_2O$ shows that the additional three bands at 1720, 1230, and 960 cm^{-1} are due more to HCOOH than to the protonated phosphate ions.

In the region of stretching OH vibrations, the IR spectrum of the LiNi precursor consists of four bands with positions close to those of $Ni(HCOO)_2{\cdot}2H_2O$. For the sake of comparison, we shall mention that the stretching OH vibrations for $LiHCOO{\cdot}H_2O$ appear at 3398 and 3109 cm^{-1}.[13] It seems that water molecules are predominantly coordinated to the nickel ions.

In summary, two features concerning the manner of coordination of the phosphate and formate groups and water molecules in $LiNiPO_4H_x(HCOO)_x{\cdot}yH_2O$ precursors can be outlined. It appears that the formate and phosphate groups are mainly deprotonated. The formate groups and water molecules prefer to coordinate around the Ni^{2+} ions, whereas the phosphate groups prefer to coordinate around the Li^+ ions. This is a specific feature of LiNi precursors obtained by freeze drying of mixed formate–phosphate solutions. When the same freeze drying method is used for the preparation of LiM–phosphate–formate (M = Fe, Mn, Co) compositions, both formate and phosphate groups are protonated, and they are coordinated to the Fe^{2+} and Li^+ ions in a nonpreferential way.[9,10,18] The different types of coordinations of PO_4^{3-} and $HCOO^-$ to M^{2+} and Li^+ in the phosphate–formate precursors determines their different thermal behavior.

Thermal decomposition of LiNi–phosphate–formate precursors leads to the formation of a target $LiNiPO_4$ composition at temperature higher than 450 °C. To elucidate the mechanism of $LiNiPO_4$ formation, Figure 2 shows the XRD patterns of the lithium–nickel–phosphate–formate precursor heated at selected temperatures in the range of 350 to 750 °C. At 350 °C, the sample is still amorphous. However, XRD peaks due to Li_3PO_4 (JCPDS 25–1030) and hexagonal Ni metal (JCPDS 45–1027) become visible. Going from 350 to 400 °C, new phases such as NiO (JCPDS 4–835) and $Li_4P_2O_7$ (JCPDS 87–409) also crystallize. This means that at 350–400 °C the thermal decomposition of freeze-dried LiNi–formate–phosphate precursors yields a mixture between Ni/NiO and lithium phosphate phases. For comparison, in this temperature range, pure $LiFePO_4$ with an olivine-type structure is obtained. This results from the different structures of the precursors. When PO_4^{3-} and $HCOO^-$ ions are preferentially coordinated around the Li^+ and Ni^{2+} ions, respectively, then mixtures of lithium phosphates and metal phases are obtained during thermal decomposition.

Structural parameters of both modifications were determined by Rietveld analysis of the XRD pattern of lithium nickel phosphate obtained at 500 °C (Figure 3).

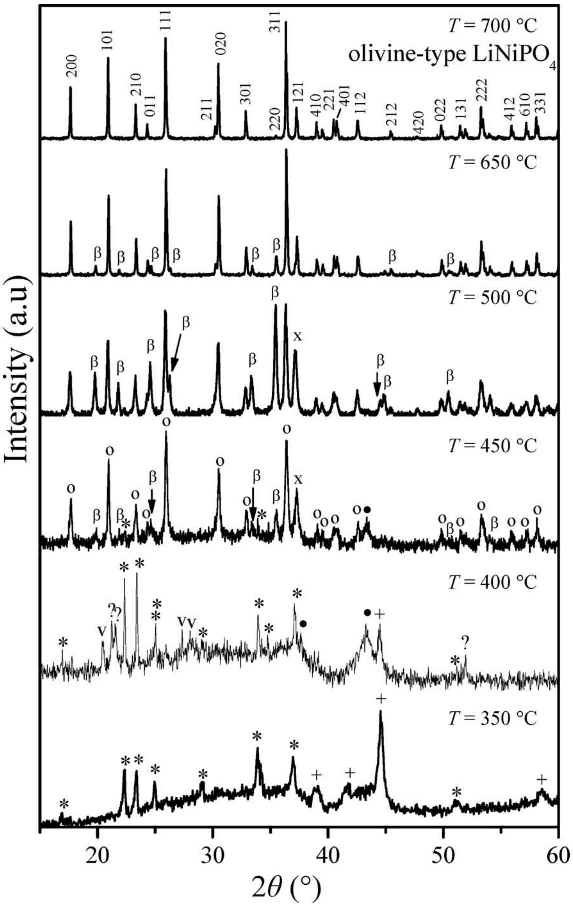

Figure 2. XRD patterns of LiNi–phosphate–formate precursor annealed at different temperatures. Symbols: Li_3PO_4 (*), metal Ni (+), NiO (●), $Li_4P_2O_7$ (v), unknown phase (?), Na_2CrO_4-type $LiNiPO_4$ (β), olivine-type $LiNiPO_4$ (o), common peak (x).

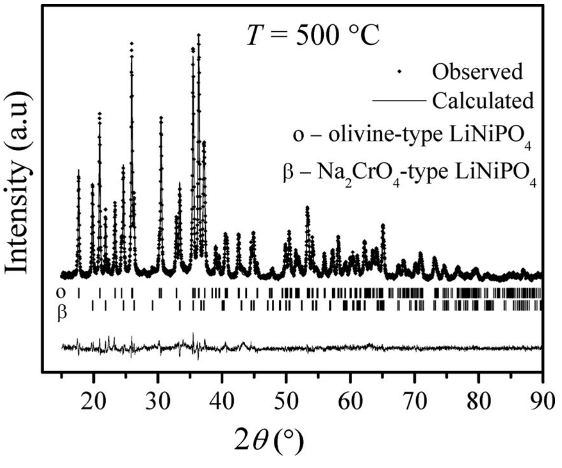

Figure 3. Rietveld refinement of the XRD pattern of lithium nickel phosphate obtained at 500 °C. Bragg reflections for olivine-type $LiNiPO_4$ (o) and Na_2CrO_4-type $LiNiPO_4$ (β) are shown. The difference between the observed and calculated profiles is plotted.

The atomic coordinates of olivine-type $LiNiPO_4$ and the high-pressure form of Na_2CrO_4-type $LiNiPO_4$ determined in ref.[8] were used as a starting model for Rietveld refinement. The structural parameters are listed in Table 1. It is worth mentioning that the lattice parameters of the Na_2CrO_4 form obtained by us at ambient pressure are close to those for the phase obtained under high pressure (6.5 GPa).[8] In addition, the lattice volume is expanded by 2.9% during the transformation from the Na_2CrO_4 form to the olivine form at ambient pressure. Under high pressure the change in the lattice volumes is 2.8%.[8]

Table 1. Structural parameters of olivine-type and Na_2CrO_4-type $LiNiPO_4$ determined from Rietveld analysis of the XRD pattern of a sample annealed at 500 °C.

	Olivine-type $LiNiPO_4$ (this work)	Na_2CrO_4-type $LiNiPO_4$, ambient pressure (this work)	Na_2CrO_4-type $LiNiPO_4$, high pressure (6.5 GPa)[8]
a [Å]	10.0426(3)	5.3628(3)	5.3580(2)
b [Å]	5.8582(2)	8.1344(3)	8.1272(3)
c [Å]	4.6804(2)	6.1279(2)	6.1241(3)
V [Å^3]	275.364(17)	267.325(17)	266.7(1)
SG	*Pnma*	*Cmcm*	*Cmcm*
Z	4	4	4
R_B	0.043	0.041	0.033
R_F	0.033	0.031	
R_{exp}	0.024	0.024	0.028
R_{wp}	0.10	0.10	0.09
χ^2	2.49	2.49	5.7

Two structural modifications are, further on, characterized by IR spectroscopy (Figure 4). The sample annealed at 700 °C exhibits a typical IR spectrum for well-crystallized olivine-type $LiNiPO_4$.[14,19] The band at 943 cm^{-1} is due to $\nu_1(PO_4)$, the bands in the region of 1147–980 correspond to $\nu_3(PO_4)$, and those in the region of 662–550 cm^{-1} correspond to $\nu_4(PO_4)$ vibrations. The bands at 525 and 476 cm^{-1} are suggested to originate mainly from Li^+ translations.[19] In the IR spectra of the samples annealed at 500 °C three additional bands are observed at 934, 609, and 501 cm^{-1}, which are attributed to the Na_2CrO_4-type form. According to factor group analysis, these bands are assigned as follows: the band at 934 cm^{-1} to the ν_1 mode, that at 609 cm^{-1} as a component from $\nu_4(PO_4)$ vibrations, and that at 501 cm^{-1} as originating from $\nu_2(PO_4)$ and/or Li^+ and Ni^{2+} translations.

The formation of the Na_2CrO_4-like modification at ambient pressure was unexpected if we take into account the previously reported data on high-pressure synthesis of the $LiNiPO_4$ modification.[8] Evidently, under the conditions of our experiments the Na_2CrO_4-type modification obtained is a metastable phase, which transforms upon heating at $T > 650$ °C into thermodynamically stable olivine modification. To prove the phase transformation, a DSC experiment was performed on a sample annealed at 500 °C (Figure 5). A broad exothermic peak between 580 and 650 °C was clearly resolved due to the Na_2CrO_4-type→olivine-type transformation. The experimentally measured enthalpy of this process was –19.1 kJ mol^{-1} for the mixture containing Na_2CrO_4-type and olivine-type $LiNiPO_4$ in a ratio of 0.44:0.56 (determined by Rietveld analysis). The recalculated enthalpy for the phase transformation of pure Na_2CrO_4-type to olivine-type $LiNiPO_4$ was ΔH = –43.40 kJ mol^{-1}.

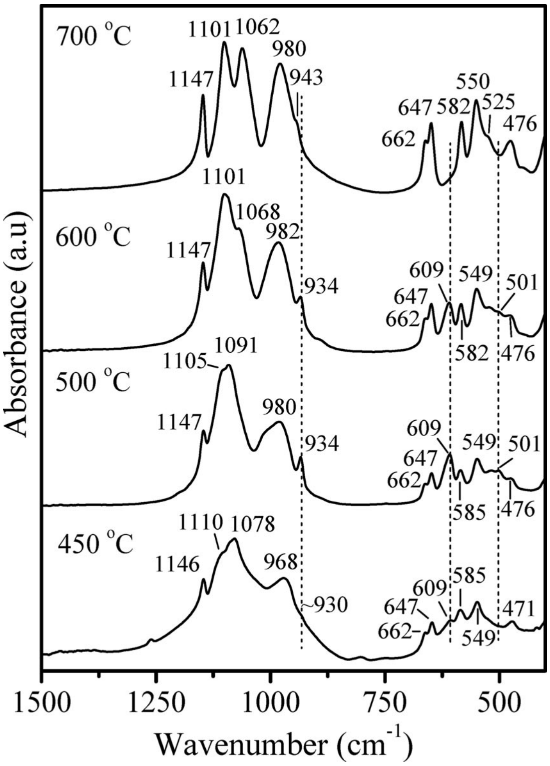

Figure 4. IR spectra of LiNi–phosphate–formate precursor annealed at different temperatures.

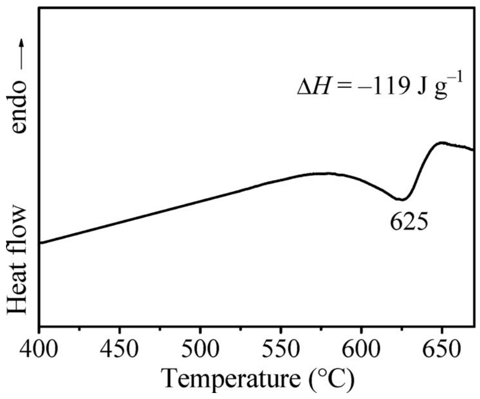

Figure 5. DSC curve of lithium nickel phosphate obtained at 500 °C (mixture of olivine-type $LiNiPO_4$ and Na_2CrO_4-type $LiNiPO_4$ in a ratio of 0.56:0.44).

For the iron, cobalt, and nickel members of the $LiMPO_4$ family, it is worth mentioning that both Na_2CrO_4-type and olivine-type forms exhibit common structural features with respect to the "metallic" framework arrangement (Li, M, and P).[8] In Figure 6 the arrangement of the cations in the two types of structures is depicted for $LiNiPO_4$. In both structures, hexagonal sheets composed of P atoms and Li/Ni atoms are ordered in an ABAB sequence. In the olivine phase, the hexagonal sheets consist of P and Ni atoms, whereas in the Na_2CrO_4 phase these sheets are formed by P and Li atoms (Figure 6). In both cases, the P atoms from two neighboring sheets build distorted octahedra, which are occupied either by Ni (Na_2CrO_4 phase, Figure 6a) or by Li (olivine phase, Figure 6b). Irrespective of this structural similarity, the formation of the Na_2CrO_4-type phase is observed for the Ni analogues only.

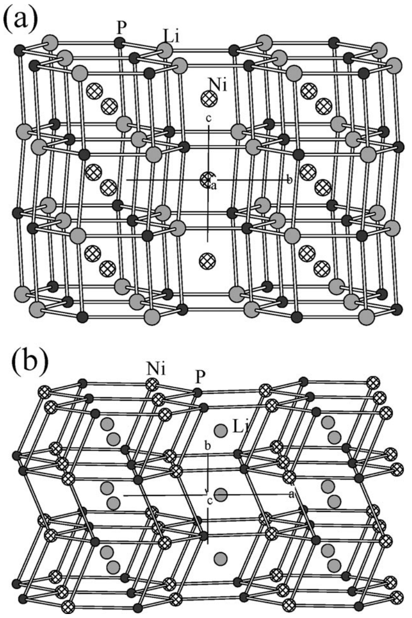

Figure 6. Structure of the metal sheets in Na_2CrO_4-type $LiNiPO_4$ (a) and olivine-type $LiNiPO_4$ (b).

The simultaneous appearance of the two structural modifications of $LiNiPO_4$ after the solid-state reaction between lithium phosphates and Ni/NiO at 450 °C allows the mechanism of their formation to be explained. On the basis of the available reports in the literature,[6,8,20,21] the preparation of the thermodynamically stable olivine-type $LiNiPO_4$ is realized at temperatures higher than 750 °C, even in the case when solution-based methods are used. This temperature is significantly higher than that of the Fe- (350 °C[9]), Mn- (450 °C[10]), and Co- (450 °C[18]) analogues. The formation of the olivine-type $LiNiPO_4$ at higher temperature implies some kinetics limitations. It appears that these kinetic difficulties give rise to the formation of the Na_2CrO_4-type metastable $LiNiPO_4$ at low temperature and ambient pressure.

Conclusions

Freeze drying solutions containing $Ni(HCOO)_2$ and LiH_2PO_4 yields precursors with compositions $LiNiPO_4H_x(HCOO)_x{\cdot}yH_2O$ ($x \approx 1.2$ and $y \approx 2.5$). In the precursor, the formate and phosphate ions are mainly deprotonated and exhibit preferential coordination: Li^+ prefers phosphate ions, whereas Ni^{2+} prefers formate ions. Below 400 °C the thermal decomposition of the precursors results in the formation of a mixture of lithium phosphates and Ni/NiO. After further annealing, two structural modifications of $LiNiPO_4$ are simultaneously formed. A Na_2CrO_4-type $LiNiPO_4$ is stabilized as a metastable phase at 450 °C, whereas pure olivine-type $LiNiPO_4$ is obtained at 700 °C. The lattice parameters of Na_2CrO_4-type $LiNiPO_4$ obtained at ambient pressure are close to that of Na_2CrO_4-type $LiNiPO_4$ obtained at high pressure (6.5 GPa). The enthalpy of the phase transition Na_2CrO_4-type → olivine-type $LiNiPO_4$ is $\Delta H = -43.40\ \mathrm{kJ\,mol^{-1}}$. Within the $LiMPO_4$ family (M = Fe, Co, Mn, Ni), the appearance of the metastable Na_2CrO_4-type modification at ambient pressure is a specific feature of the Ni analogue. The much higher temperature of formation of the olivine-type $LiNiPO_4$ (700 °C) as compared to the Co and Fe olivines (350–450 °C) is most probably a consequence of kinetic limitations.

Experimental Section

The homogeneous lithium–nickel–phosphate–formate precursors were prepared following the procedure developed earlier for the iron and manganese compounds, respectively.[9,10]

Transparent phosphate–formate solutions of lithium and nickel were obtained by mixing solutions of $Ni(HCOO)_2{\cdot}2H_2O$ and LiH_2PO_4, keeping a stoichiometric 1:1:1 = Ni/Li/P ratio. The pH value of both solutions before mixing was adjusted to pH ≈ 3 with addition of a small quantity of HCOOH (1:1). Solutions with concentrations of 0.05 and 0.1 M with respect to the metal ions were prepared. As-prepared solutions were frozen instantly with liquid nitrogen and dried in vacuo (20–30 mbar) at –20 °C with an Alpha-Christ Freeze Dryer. After drying, the solid precursors were predecomposed at 350 °C for 3 h and then further annealed at temperatures from 350 to 750 °C for 10 h under a static air atmosphere.

The starting $Ni(HCOO)_2{\cdot}2H_2O$ was prepared by dissolving nickel carbonate with dilute formic acid at 60–70 °C. The solution was then filtered and concentrated. Crystals were obtained by cooling to room temperature. $Ni(HCOO)_2{\cdot}2H_2O$ is very stable during storage, which ensures an exact stoichiometry in the final product.

The chemical composition of the precursors and of the $LiNiPO_4$ samples was determined by using data from the chemical analyses of Ni (complexometrically), Li (atomic absorption analysis), C and H (Elementar Analysensysteme GmbH), and thermal analysis ("Stanton Redcroft" apparatus). X-ray structural analysis was made with a Bruker Advance 8 diffractometer (Cu-K_α radiation). Step-scan recordings for structure refinement by the Rietveld method were carried out using by 0.02° 2θ steps of 10 s duration. The computer program FULLPROF was used in the calculations. The DSC curve was recorded using DSC 20 of Mettler TA 3000 system at a heating rate of $10\ \mathrm{°C\,min^{-1}}$.

Acknowledgments

Authors are grateful for the financial support of the National Science Fund of Bulgaria (Ch 1701/2007) and to the National Centre for New Materials (DO-02-82/2008). Thanks to Prof. T. Spassov (Sofia University, Bulgaria) for the DSC measurement.

---

[1] A. S. Anderson, J. O. Thomas, *J. Power Sources* **2001**, *97–98*, 498–502.
[2] A. K. Padhi, K. S. Nanjuindaswamy, J. B. Goodenough, *J. Electrochem. Soc.* **1997**, *144*, 1188–1194.
[3] M. S. Whittingham, Y. Song, S. Lutta, P. Y. Zavalij, N. Chernova, *J. Mater. Chem.* **2005**, *15*, 3362–3379.
[4] G. Li, H. Azuma, M. Tohda, *Electrochem. Solid-State Lett.* **2002**, *5*, A135–137.
[5] K. Amine, H. Yasuda, M. Yamachi, *Electrochem. Solid-State Lett.* **2000**, *3*, 178–179.
[6] J. Wolfenstine, J. Allen, *J. Power Sources* **2005**, *14*, 389–390.
[7] U. Amador, J. M. Gallardo-Amores, G. Neymann, H. Huppertz, E. Morán, M. E. Arroyo y de Dompablo, *Solid State Sci.* **2009**, *1*, 343–348.
[8] O. García-Moreno, M. Alvarez-Vega, F. García-Alvarado, J. García-Jaca, J. M. Gallardo-Amores, M. L. Sanjuán, U. Amador, *Chem. Mater.* **2001**, *13*, 1570–1576.
[9] V. Koleva, E. Zhecheva, R. Stoyanova, *J. Alloys Compd.* **2009**, *476*, 950–957.
[10] V. Koleva, R. Stoyanova, E. Zhecheva, *Mater. Chem. Phys.*, submitted.
[11] K. G. Kidd, H. H. Mantsch, *J. Mol. Spectrosc.* **1981**, *85*, 375–389.
[12] A. Heyns, *J. Mol. Struct.* **1985**, *127*, 9–20.
[13] K. Mouaïne, P. Becker, C. Carabatos-Nédelec, *Phys. Status Solidi B* **1997**, *200*, 273–287.
[14] A. Ait Salah, P. Jozwiak, K. Zaghib, J. Garbarczyk, F. Gendron, A. Manger, C. M. Julien, *Spectrochim. Acta* **2006**, *65A*, 1007–1113.
[15] A. Novak, *Struct. Bonding (Berlin)* **1974**, *18*, 177–216.
[16] J. Baran, T. Lis, M. Drozd, H. Ratajczak, *J. Mol. Struct.* **2000**, *516*, 185–202.
[17] J. Xu, D. F. R. Gilson, I. S. Butler, *Spectrochim. Acta Part A* **1998**, *54*, 1869–1878.
[18] V. Koleva, E. Zhecheva, R. Stoyanova, *unpublished data*.
[19] M. Th. Paques-Ledent, P. Tarte, *Spectrochim. Acta Part A* **1974**, *30*, 673–689.
[20] K. Rissouli, K. Benkhouja, J. R. Ramos-Barrado, C. Julien, *Mater. Sci. Eng.* **2003**, *B98*, 185–189.
[21] Gangulibabu, D. Bhuvaneswari, N. Kalaiselvi, N. Jayaprakash, P. Periasamy, *J. Sol-Gel Sci. Technol.* **2009**, *49*, 137–144.

Received: July 28, 2009